

## Nanostructured polyelectrolyte multilayer drug delivery systems for buccal administration

M. Marudova<sup>1\*</sup>, I. Bodurov<sup>1</sup>, S. Sotirov<sup>1</sup>, Y. Uzunova<sup>2</sup>, B. Pilicheva<sup>2</sup>, I. Avramova<sup>3</sup>, A. Viraneva<sup>1</sup>, I. Vlaeva<sup>4</sup>, G. Exner<sup>1</sup>, T. Yovcheva<sup>1</sup>

<sup>1</sup>Plovdiv University "P. Hilendarski", Faculty of Physics, 24 Tsar Assen str., Plovdiv, Bulgaria

<sup>2</sup>Medical University Plovdiv, Faculty of Pharmacy, 15A Vassil Aprilov Blvd., Plovdiv, Bulgaria

<sup>3</sup>Institute of General and Inorganic Chemistry, Bulgarian Academy of Sciences, Acad. G. Bonchev Blvd., Block 11, Sofia, Bulgaria

<sup>4</sup>University of Food Technologies, 26 Maritsa Blvd., Plovdiv, Bulgaria

Polyelectrolyte multilayers (PEMs) are well-defined nanoarchitectures with many potential applications, usually as biomaterial coatings. They possess excellent characteristics, such as fine tuning of thickness, stiffness, stability, morphology and topography. Hence they may exhibit special biological properties, such as mucoadhesion and local drug delivery. We present our recent investigations on layer-by-layer assembled polyelectrolyte multilayers from chitosan and xanthan on preliminary corona charged substrates from poly- $\epsilon$ -caprolacton. Polyelectrolyte multilayers were deposited by two different techniques – dip-coating and spin-coating. The presence of PEMs on the substrates was proved by ATR FT-IR spectroscopy. The surface chemical composition was established by X-ray photoelectron spectroscopy (XPS). Further investigations on the morphology and topography of the samples were done by scanning electron microscopy (SEM) and atomic force microscopy (AFM). All the experimental data confirmed differences in the structure and surface properties of the PEMs assembled by dip-coating and spin-coating. An interdiffusion of the polyelectrolyte layers was observed in dip-coated PEMs, while flat and clearly separated layers were deposited by spin-coating. The ability to control the inner structure of the PEMs enables to manipulate the physical properties or chemical activity of the functionalized thin films. In this way tunable mucoadhesion and drug release properties could be achieved.

**Keywords:** polyelectrolyte multilayers, drug delivery, mucoadhesion, chitosan, xanthan, charged poly- $\epsilon$ -caprolacton substrates

### INTRODUCTION

The fabrication of thin polyelectrolyte layers by the electrostatic assembly of oppositely charged polyelectrolytes (LbL self-assembly) has recently attracted much interest [1, 2]. The formation of these films is electrostatically driven, and favoured by the release of counterions. During the assembly, polyelectrolytes from solutions form electrostatically bound complexes with polyelectrolyte functional groups of opposite charges that are present on the surface, leaving excess charges upon adsorption due to charge overcompensation. Therefore, the surface charge of the outermost layer is altered between the anionic and cationic state, and this charge reversal offers a driving force for the sequential build-up of multilayers in the assembly. As a result, one can obtain a more or less irreversibly adsorbed polyelectrolyte multilayer of which thickness and interpenetration can be readily manipulated with varying the type of adsorbing species, type of deposition technique and processing conditions such as polyelectrolyte charge, ionic strength, salt concentration and adsorption time [3-5].

LbL self-assembly usually leads to a linear growth of film thickness [6, 7]. However, some authors have reported cases of LbL assemblies in which the film thickness grows exponentially with increasing the number of polyelectrolyte deposition layers [8, 9]. Usually this phenomenon is observed for weakly charged polyelectrolyte multilayer systems. It can be attributed to the reversible interdiffusion of at least one of the polyelectrolyte species that constitute the film.

Structure and topography of LbL assemblies influence properties such as adhesion, biocompatibility, and drug release [10]. Quantitative characterization of the multilayers surfaces made from various polymer components is important both for practical purposes e.g. for evaluating the biocompatibility, and for the comparison of the influence of the polymer constituents on the multilayer features.

The aim of the present study is characterisation of the chemical composition, structure and surface topography of weak polyelectrolyte multilayers from chitosan and xanthan on biodegradable substrates in respect to their use for buccal drug delivery.

\* To whom all correspondence should be sent:  
margo@uni-plovdiv.bg

## EXPERIMENTAL

### *Substrate formation*

Poly( $\epsilon$ -caprolacton) (PEC) with ester end groups and intrinsic viscosity (1-1.3) dL/g was purchased from Lactel Absorbable Polymers (USA) and used for the preparation of biodegradable substrates. The PEC substrates were casted from 2% w/v PEC solution in chloroform and dried at 35°C for 48 hours. Their thickness was (40  $\pm$  5)  $\mu$ m. They were then kept in an exicator, at room temperature, and 54% relative humidity (RH). Before the deposition process, the substrates were charged in a corona discharge system, consisting of a corona electrode (needle), a grounded plate electrode and a metal grid placed between them. A voltage of  $\pm$  5 kV was applied to the corona electrode and a voltage of  $\pm$  1 kV to the grid. The polarity of the corona electrode and the grid electrode was one and the same. The samples were charged under standard room conditions (T = (21 $\div$ 23) °C and RH = 45-55%) for 1 minute.

### *Polyelectrolyte multilayers deposition*

Layer-by-layer (LbL) deposition technique was applied for multilayer build-up. Chitosan (low molecular weight) and xanthan gum were purchased from Sigma-Aldrich and were used without further purification or characterization. For the LbL assembly 0.1% w/v chitosan and 0.05% w/v xanthan solutions in acetate buffer (pH 4.5 and ionic strength 0.1 M) were prepared. The deposition was done in two ways – dip-coating and spin-coating. In both cases, the first built-up layer always possessed opposite to the substrate electric charge.

For dip-coating assembly a slide stainer (Poly Stainer IUL, Spain) was used with the deposition program: 15 min adsorption of polyelectrolyte solution, followed by 5 min washing step in the acetate buffer. The procedure was repeated until reaching the desired even numbers of layers (8, 14 or 20 xanthan/chitosan or chitosan/xanthan). After the last layer deposition the film was dried with hot air.

For the spin-coating assembly a DDR Labortechnik T54 spin-coater was used. Polyelectrolyte solutions of chitosan and xanthan were alternately spun coated (15 s at 1000 rpm) onto the preliminary charged substrates with an intermediate washing step (acetate buffer) before the deposition of each consecutive layer.

Ready multilayer structures were stored in an exicator at RH 54%.

### *ATR-FTIR spectroscopy*

The ATR-FTIR spectra were collected by means of a Thermo Scientific™ Nicolet™ iSTM 10 FT-IR spectrometer, equipped with a diamond ATR accessory in the range (650-4000)  $\text{cm}^{-1}$ , giving a 4  $\text{cm}^{-1}$  resolution and 64 scans. The integral intensity was measured using an OMNIC software package.

### *XPS analysis*

The X-ray photoelectron spectroscopy was used for investigation of the surface chemical states of polyelectrolyte multilayers. For that purpose an Axis Supra (Kratos Analytical Ltd, GB) electron spectrometer was used. The survey, C1s, O1s, and N1s photoelectron lines had been recorded with monochromatic Al K $\alpha$  radiation (1486.6 eV) under 10<sup>-7</sup> Pa base pressure and total instrumental resolution of  $\sim$ 0.48 eV. The binding energies (BE) were determined utilizing the C1s line (from an adventitious carbon) as a reference with energy of 285.0 eV. All data were recorded at a 90° take-off angle. High resolution C1s, O1s, N1s, F1s, Na1s, S2p, Si2p spectra were collected at a pass energy of 20 eV. The concentration of the elements on the surface of polymers had been calculated.

### *Scanning electron microscopy (SEM)*

The morphology of the obtained polyelectrolyte multilayer structures was examined by means of SEM. A scanning electron microscope Lyra 3 XMU (Tescan) was employed. The working voltage was 30 kV. Prior to the measurements, the samples were covered with a thin film of gold (about 30 nm).

### *Atomic force microscopy (AFM)*

The polyelectrolyte multilayer topography was analysed by a Nanosurf Flex AFM (Switzerland). The surface images were obtained in tapping mode with a standard cantilever Tap190A1-G with a 10 nm tip radius. The viewing field consisted of 256x256 pixels, revealing the morphology of a 10  $\mu$ m x 10  $\mu$ m area from the sample surface. The line scan time was 1 s. Based on the AFM images, the surface roughness and PSD spectra were calculated using a Gwyddion software.

## RESULTS AND DISCUSSION

Attenuated total reflection (ATR) FT-IR spectroscopy was used to confirm the polyelectrolyte deposition. Typical spectra of positively and negatively charged substrates with 8, 14 and 20 polyelectrolyte layers deposited by dip-coating assembly are shown in the Fig.1 and Fig.2. Slightly intense bands of CH groups stretching

vibrations at  $2880\text{ cm}^{-1}$  and  $2946\text{ cm}^{-1}$  are observed in both substrate and polyelectrolyte multilayers spectra. The broad band between  $3000$  and  $3700\text{ cm}^{-1}$  is due to a combination of two vibrations: OH groups and amine groups, which is present in the chitosan [11]. A band at  $1594\text{ cm}^{-1}$ , which corresponds to an amino group [12], is present only in the spectra of the polyelectrolyte multilayer structures and its intensity increases with increasing the number of the deposited layers.

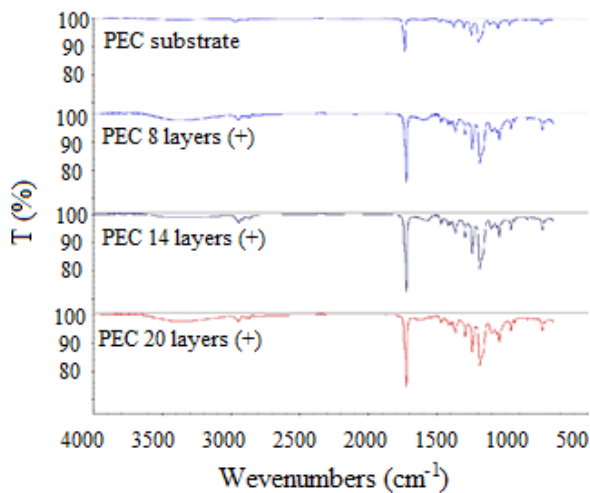


**Fig.1.** ATR FT-IR spectra of xanthan/chitosan multilayers deposited on positively charged PEC substrate

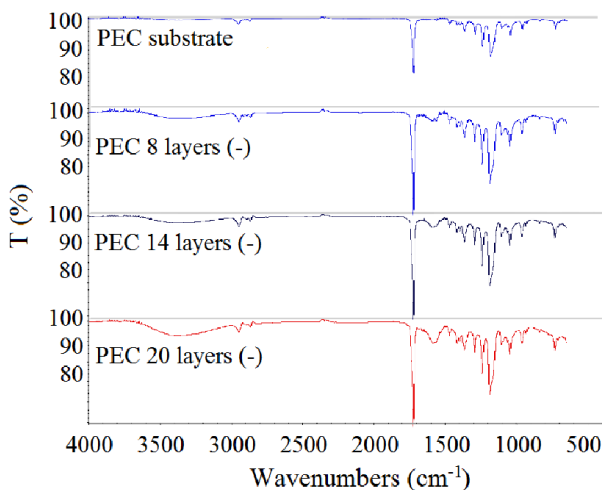


**Fig.2.** ATR FT-IR spectra of chitosan/xanthan multilayers deposited on negatively charged PEC substrate

Peaks corresponding to the vibrations of  $\text{NH}_3^+$  ( $1632\text{ cm}^{-1}$  and  $1522\text{ cm}^{-1}$ ) of chitosan and ionized carboxyl group ( $\text{COO}^-$ ) of xanthan at  $1620\text{ cm}^{-1}$  are not observed in the spectra, which suggests the formation of a complex between the deposited polyelectrolytes by ionic interactions between the

$\text{NH}_3^+$  groups of chitosan and ionized carboxyl group  $\text{COO}^-$  of xanthan [13].

Similar ATR-FTIR spectra were collected for xanthan/chitosan multilayers, assembled by spin-coating (the data are not shown). In that case the peak intensities were less pronounced than these for the dip-coated samples.

Based on the ATR-FTIR analysis the following conclusions can be derived:

- Both dip-coating and spin-coating assemblies lead to irreversible deposition of xanthan and chitosan on pre-charged PEC substrates.
- The increase of the number of layers leads to a higher amount of deposited hydrocolloids.
- Chitosan and xanthan molecules interact predominantly by ionic interactions to form polyelectrolyte complexes.

Further investigations on the surface chemical composition of the polyelectrolyte multilayers were done by X-ray photoelectron spectroscopy (XPS). The N1s spectra, collected from the surfaces of multilayers, assembled by dip-coating and spin-coating on both positively and negatively charged substrate (i.e. structures finishing with chitosan or xanthan layer respectively) are shown in Fig.3a and Fig.3b.

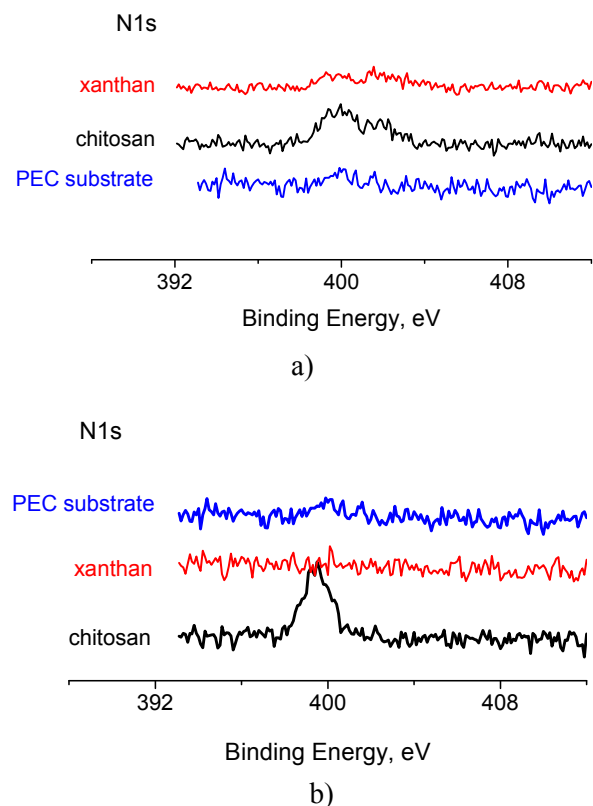


**Fig.3.** N1s XPS spectra of polyelectrolyte multilayers, assembled by dip-coating (a) and spin-coating (b)

Quantity analysis of the nitrogen concentration on the multilayer surfaces is presented in Table 1.

As nitrogen appears just in the structure of chitosan, the following conclusions can be derived:

**Table 1.** Nitrogen surface atomic concentration of chitosan/xanthan polyelectrolyte multilayers

Atomic concentration [%]	Dip-coating		Spin-coating	
	Chitosan	Xanthan	Chitosan	Xanthan
Last layer Nitrogen	1.95	1.93	0.69	0.00

- The amount of the deposited polyelectrolytes is bigger in the case of the dip-coating assembly.
- Diffusion of chitosan and interlayer penetration is observed in the polyelectrolyte multilayer structures, assembled by dip-coating. This is

the reason that nitrogen appears on the surface of structures finishing with a xanthan layer.

- There is no nitrogen detected in the xanthan layer in the spin-coated samples, therefore no interpenetration is observed and clear separated layers were formed.

These observations are in agreement with previous investigations on the deposition process of weakly charged polyelectrolytes [14, 15]. Shear forces arising during the spin-coating assembly lead to smaller amounts of adsorbed polyelectrolytes within LbL films, resulting in a higher degree of internal film order, and dramatically improved stability of assemblies in salt solutions as compared to dip-coated LbL assemblies.

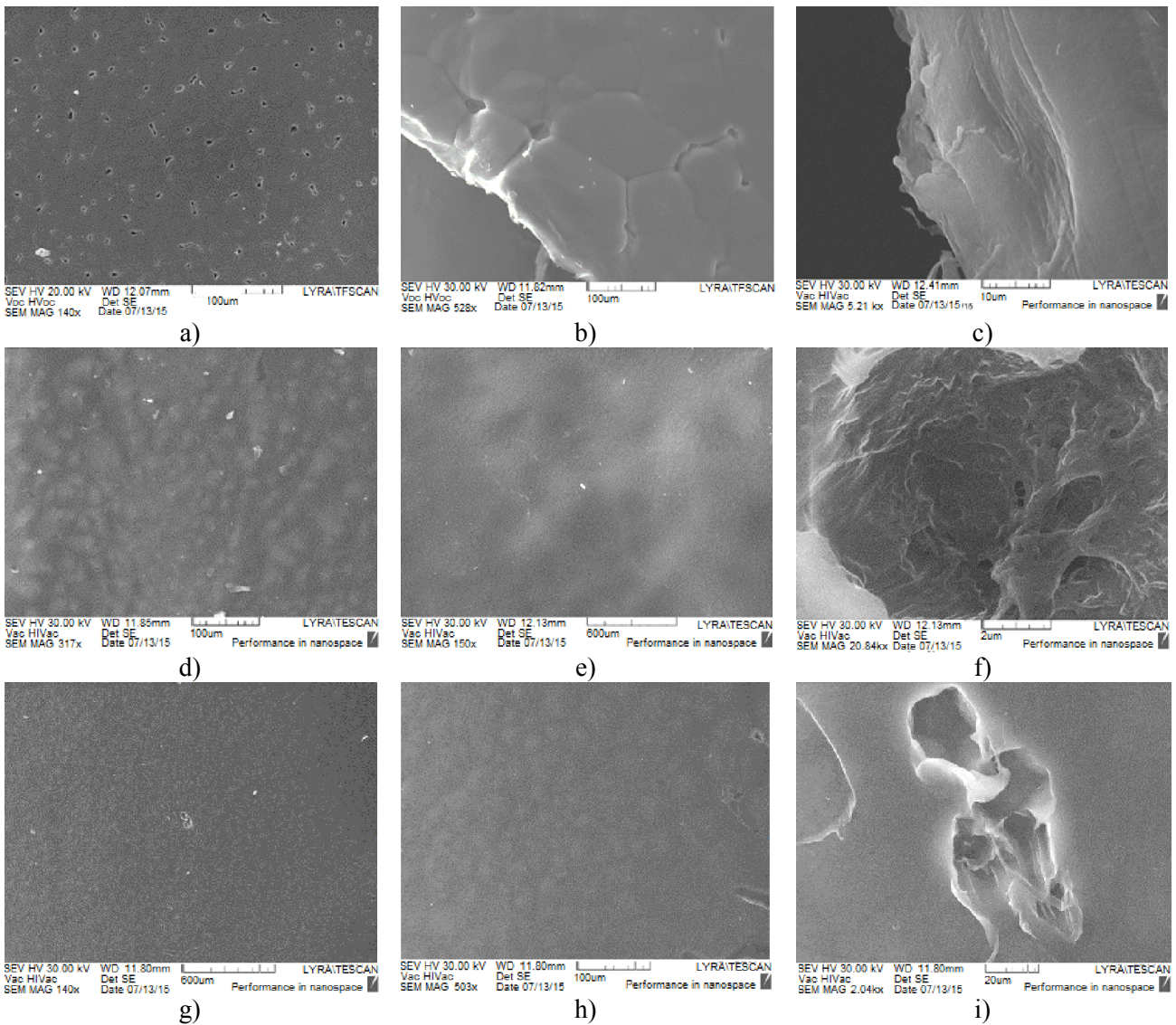


**Fig.4.** SEM micrographs of PEC substrates (a-c); PEC substrates, coated with 10 (d) and 20 (e, f) layers, ending with xanthan; PEC substrates, coated with 10 (g) and 20 (h, i) layers, ending with chitosan

The surface morphology of the PEC substrates and dip-coated chitosan/xanthan polyelectrolyte multilayers with different number of layers and different end layers are presented in Fig.4.

It is important initially to study the morphology of the substrate, since it largely determines the mode and the type of the deposited thereon thin layers.

During the fabrication of the poly ( $\epsilon$ -caprolactone) substrate from solution, the long time for evaporation of the solvent facilitates the preparation of large (size of about 200  $\mu\text{m}$ ) spherulites (Fig.4a-b). Spherulites are composed of lamellae, which are well observed at larger magnifications (Fig.4c).

LbL deposition of the polyelectrolyte layers by dip-coating on a negatively charged substrate leads to a gradual change of the morphology of the surface thereby the general characteristics of the substrate are retained (Fig.4d-f). In case of a negatively charged substrate (multilayers ending with xanthan) the morphological units increase in size by increasing the number of layers – Fig.4d-e. This interesting finding is explained by the porous

structure of the deposited chitosan/xanthan complexes – Fig.4f. Porous complexes are typical for stiff macromolecules like xanthan. The observation is in agreement with the reported one in the literature data about a toroid morphology of xanthan/chitosan complexes reported [16]. Significant difference is observed in positively charged substrates (multilayers ending with chitosan, where the morphological units remain the same size, even at 20 deposited layers – Fig.4g-h). As shown in the Fig.4i the morphology of the deposited complexes in that case is dense lamella.

Presented microphotographs show the successful deposition of polyelectrolyte multilayer structures on PEC substrates. The observed differences in the morphology could be relevant to the different size and flexibility of xanthan and chitosan, which resulted in varied extent of macromolecular interdiffusion and multilayer penetration.

More detailed analysis of the surface topography was carried out by AFM for samples with various number of polyelectrolyte layers - Fig.5.

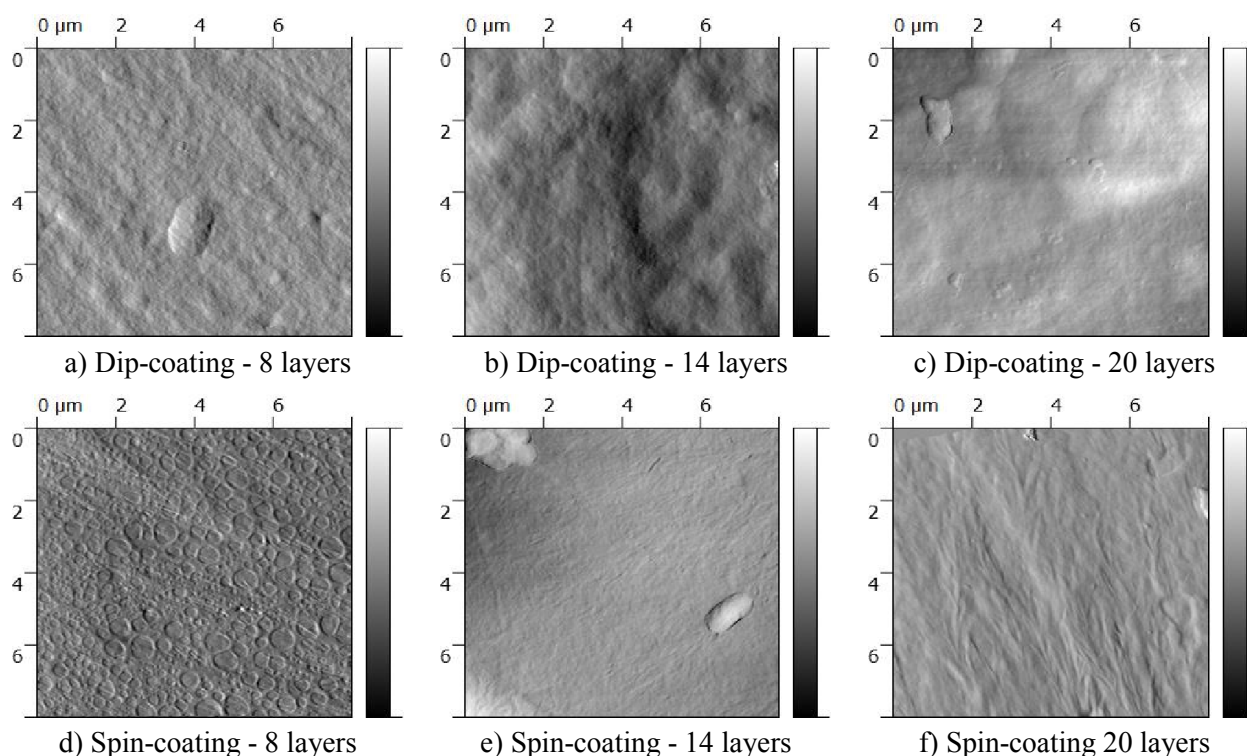


**Fig.5.** AFM micrographs of polyelectrolyte multilayers ending with xanthan, which are deposited by dip-coating (a-c) and spin-coating (d-f) technique

The polyelectrolytes, which are deposited by dip-coating technique, revealed a network-like structure for all samples with different number of

layers – Fig.5a-c. However for the 20 layer samples there were additional regions on the surface where polymer had accumulated on the top of the network

structure – Fig.5c. The dimensions of the network voids increased in size with the increase of the number of layers.

The polyelectrolytes, which are deposited by spin-coating, revealed a pattern structure, which is more pronounced for 14 and 20 layers samples – Fig.5e-f. Most probably it is related to molecular orientation due to the centrifugal forces.

Based on the AFM micrographs the following conclusions could be formulated:

- The surface roughness Rms shows an increase with the increase of the numbers of deposited layers for both deposition techniques – Table 2. This is similar to the trend reported for similar systems [17, 18].
- The spin-coated layers are smoother than the dip-coated ones.

**Table 2.** Roughness of dip-assembled and spin-assembled polyelectrolyte multilayers ending with xanthan

Sample	Rms [nm]		
	8 layers	14 layers	20 layers
Dip-coating	63.2	118.3	133.2
Spin-coating	22.8	77.7	90.9

The low roughness for spin-coated samples suggested flat and clearly separated interfaces between the layers which could be interpreted as lack of interpenetration in the case of spinning assembly. On the contrary, the surfaces topography of dipping-assembled films consists of rough patterns, indicating loose interpenetrating structures.

Additional quantity analysis of the multilayer surface topography is done by evaluating the power spectral density (PSD) spectra. The PSD function is useful in analysing surface roughness. This function provides a representation of the amplitude of a surface's roughness as a function of the spatial frequency of the roughness. The dependence of PSD ( $W$ ) on the spatial frequency ( $k$ ) for dip-coated and spin-coated multilayers, ending with xanthan are presented in Fig.6.

Three different characteristic regions could be identified in the PSDs. First, the PSDs display a frequency independent plateau at low spatial frequencies. This is followed by a transition to a power law dependence at higher frequencies. Additionally, a peak at even higher frequencies was observed in the PSDs. The transition space frequency in both dip- and spin-coating mode is the same and gives the surface pore-size of about 1  $\mu\text{m}$ . Two high-frequency peaks at about 300 nm and 200 nm could be detected for the dipping-mode.

The dimensions of 200 nm and 300 nm are relevant to the xanthan radius of gyration [19] and therefore it could be assumed that in multilayers, which are deposited by dip-coating, the polyelectrolytes are in a random coil conformation. A series of peaks in the PSD spectra are recognized for the spin-assembled multilayers. Probably the pattern is due to the centrifugal force, which dominates during the deposition process.

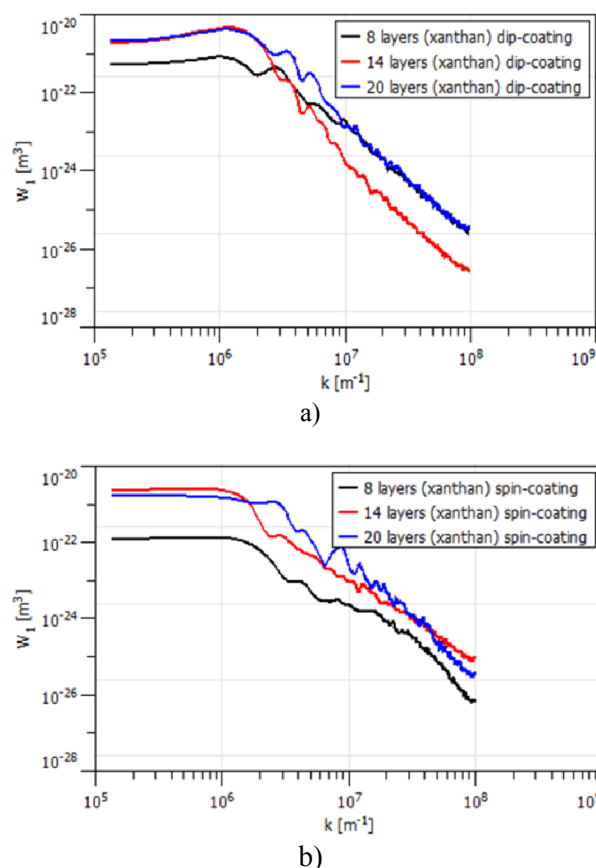


**Fig.6.** PSD spectra of dip-coated (a) and spin-coated (b) multilayers, ending with xanthan

In Fig.7 the PSD spectra of dip-coated and spin-coated samples with 20 layers ending with chitosan and xanthan respectively are compared.

The multilayers ending with xanthan are characterized with higher roughness in both coating modes. The transition frequency corresponds to surface pore-size of 1 micron. The surfaces of multilayers ending with chitosan are smoother and the pore size is about 300 nm. The observed differences could be explained by different characteristics sizes and chain flexibility of xanthan and chitosan. In case of xanthan the molecular mass is higher and the functional carboxyl groups are situated in the branches. Therefore looser network is formed.

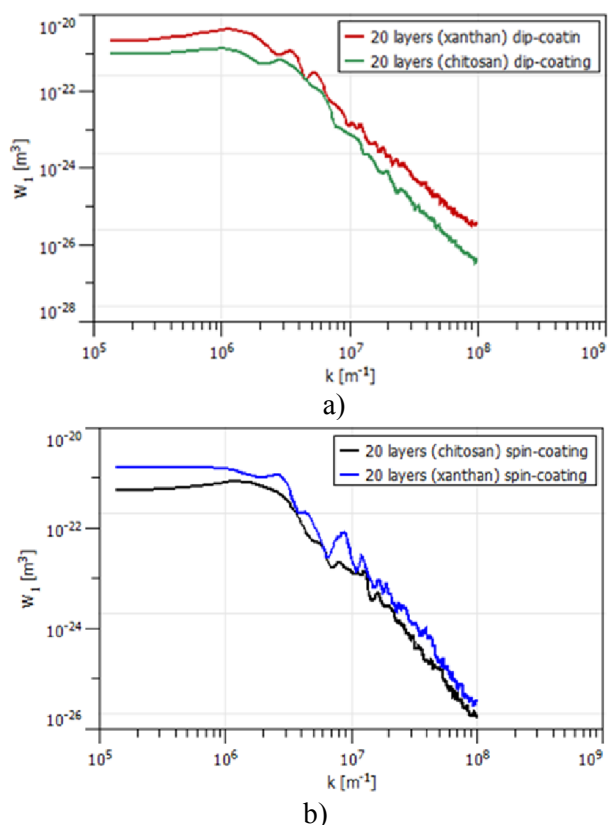


**Fig.7.** PSD spectra of dip-coated (a) and spin-coated (b) multilayers, ending with xanthan or chitosan respectively

### CONCLUSIONS

This study shows that dip-coating and spin-coating techniques are successfully applied for the deposition of chitosan and xanthan multilayers on PEC corona charged substrates. In both methods of assembly the binding of polyelectrolytes to the substrate is irreversible and multilayer growth is predominantly due to ionic interactions and formation of polyelectrolyte complexes.

The surface roughness and surface chemical compositions of dip-coating multilayers indicate the presence of inter-polymer diffusion and interpenetration. The polyelectrolytes are in random-coil conformation.

Spin-coating process causes fabrication of flat clearly separated multilayers with orientated pattern topography.

### ACNOWLEDGEMENTS

This study was financial supported by Project No DFNI B-02/7 of Bulgarian National Scientific

Fund and Project MU-15-FFIT-003/23.04.2015 of Department of Scientific Research at the Plovdiv University.

### REFERENCES

- 1 G. Decher, J.B. Schlenoff (Eds.), *Multilayer Thin Films. Sequential Assembly of Nanocomposite Materials*, 2nd Edition, Wiley-VCH, (2012).
- 2 C. Picart, F. Caruso, J.-C. Voegel, G. Decher *Layer-by-Layer Films for Biomedical Applications*, Wiley-VCH, (2014).
- 3 Y. M. Lee et al., *Journal of nanoscience and nanotechnology*, 9, 7467, (2009).
- 4 S. S. Shiratori and M. F. Rubner, *Macromolecules*, 33, 4213, (2000).
- 5 M. Losche, J. Schmitt, G. Decher, W. G. Bouwman, and K. Kjaer, *Macromolecules*, 31, 8893, (1998).
- 6 K. Glinel, A. Moussa, A. M. Jonas, and A. Laschewsky, *Langmuir*, 18, 1408, (2002).
- 7 B. Schoeler, G. Kumaraswamy, and F. Caruso, *Macromolecules*, 35, 889, (2002).
- 8 P. Lavalle, C. Gergely, F. J. G. Cuisinier, G. Decher, P. Schaaf, J. C. Voegel, and C. Picart, *Macromolecules* 35, 4458, (2002).
- 9 C. Picart, J. Mutterer, J. L. Richert, Y. Luo, G. D. Prestwich, P. Schaaf, J. C. Voegel, and P. Lavalle, *P. Natl. Acad. Sci. USA*, 99, 12531, (2002).
- 10 E. Marken, M. Gjertrud, and B. T. Stokke, *Thin Solid Films*, 516, 7770, (2008).
- 11 P. Katugampola, and W. Cherese, *International Journal of Pharmaceutical Science Invention*, 3, 24, (2014).
- 12 N. Kulkarni, P. Wakte, J. Naik, *International Journal of Pharmaceutical Investigation*, 5(2), 73, (2015).
- 13 M. Fukuda, N.A. Peppas, J.W. McGinity, *International Journal of Pharmaceutics*, 310, 90, (2006).
- 14 Y. M. Lee, D. K. Park, W-S. Choe, S. M. Cho, G. Y. Han, J. Y. Park, J. Pil, *Journal of Nanoscience and Nanotechnology*, 9, 7467, (2009).
- 15 Zhuk, Aliaksandr, et al., *Langmuir*, 31, 3889, (2015).
- 16 G. Maurstad, S. Danielsen, and B. T. Stokke, *The Journal of Physical Chemistry B*, 107, 8172, (2003).
- 17 G. Maurstad, et al., *Macromolecular Symposia*, 227, 161, (2005).
- 18 R. F. M. Lobo, M. A. Pereira-da-Silva, M. Raposo, R. M. Faria, O. N. Oliveira, *Nanotechnology*, 14, 101, (2003).
- 19 E. Dickinson, M. E. Leser (Eds.), *Food Colloids : Self-Assembly and Material Science*, Royal Society of chemistry, (2007).